JOURNAL OF CATALYSIS **161,** 254–262 (1996)
ARTICLE NO. 0183

N_2O Decomposition over Manganese Oxides

Tatsuji Yamashita and Albert Vannice[1]

Department of Chemical Engineering, The Pennsylvania State University, University Park, Pennsylvania 16802-4400

Received October 27, 1995; revised February 26, 1996; accepted March 1, 1996

The catalytic decomposition of N_2O was studied over four different oxides of manganese—MnO, Mn_3O_4, Mn_2O_3, and MnO_2. The respective specific activities were 6.3×10^{-4}, 2.5×10^{-3}, 4.8×10^{-3}, and 8.1×10^{-4} μmol/s · m^2 at 623 K and 0.066 atm of N_2O. Apparent activation energies fell between 19 and 27 kcal/mol, and the reaction orders with respect to N_2O were between 0.74 and 0.89. XRD patterns showed that pretreatment at 773 K under He converted MnO_2 into Mn_2O_3, which gave a specific activity similar to that of the original Mn_2O_3 sample; therefore, MnO_2 was pretreated under pure oxygen at 645 K prior to reaction to retain the bulk MnO_2 phase. On the other hand, MnO was oxidized to Mn_3O_4 during the course of N_2O decomposition. Thus Mn_2O_3 is the phase associated with the highest catalytic activity. A detailed kinetic study with the most active Mn_2O_3 sample found that the reaction order at 648 K with respect to N_2O was near 0.8 over a wide pressure range, and the reaction rate was retarded by oxygen. The experimental data fit a simple Langmuir–Hinshelwood model well and both kinetic and thermodynamic parameters could be determined. The activation energy for the rate determining step—dissociation of adsorbed N_2O into $N_{2(g)}$ and adsorbed oxygen—was 31 kcal/mol. Weak N_2O adsorption was indicated by heat of adsorption and entropy of adsorption values of 7 kcal/mol and -9 cal/mol · K, respectively, while for O_2 adsorption the respective values were 22 kcal/mol and -26 cal/mol · K. Independent Langmuir isotherms for N_2O adsorption between 297 and 353 K revealed only reversible adsorption with a heat of adsorption of 5 kcal/mol.

INTRODUCTION

Because of its simplicity N_2O decomposition has been used for decades as a probe to evaluate the catalytic activity and other surface properties of various solids (1). Recently, the study of this reaction has gained more significance because N_2O has been recognized as an environmental pollutant. Being produced in large amounts as a by-product from the manufacture of adipic acid as well as from industrial combustion processes, it is considered to contribute to stratospheric ozone depletion and the greenhouse effect (2, 3). N_2O has been studied over various metal oxides, mixed metal oxides, and some zeolites (4–37). Of these catalysts Rh-ZSM-5 seems to be most active (4). For N_2O decomposition over metal oxides, Dell *et al.* stressed the effect of semiconductor type, that is, p-type semiconductors show the highest activities, n-type the lowest, and insulators are intermediate (5). Winter, on the other hand, emphasized the importance of anion vacancies (6). Common to most studies on metal oxides, including the above, is the need for labile oxygen on the catalyst to complete the catalytic cycle. Manganese can have multiple oxidation states, and several phases exist as oxides in the form of MnO, Mn_3O_4, Mn_2O_3, and MnO_2, which vary in the degree of oxygen lability. Although several studies have been published on N_2O decomposition over Mn_2O_3 and MnO_2 (7–11), specific activities were not always reported and a comparative study of the catalytic behavior of this series of Mn oxides has not been conducted. This investigation examined the kinetics of N_2O decomposition over these four Mn oxides, it determined specific activities and, based on detailed kinetic data obtained with the most active Mn oxide, Mn_2O_3, the possible reaction mechanisms are discussed.

EXPERIMENTAL

The Mn oxides used as catalysts were all provided by Chemetals, Inc., and some of their properties are given in Table 1. Mn_3O_4, Mn_2O_3, and MnO_2 were powders with diameters of about 40 μm, whereas the MnO particles were somewhat larger and therefore were sieved to collect a 40- to 60-mesh portion before use. XRD patterns were obtained with a Rigaku Geigerflex diffractometer with a D_{max}-B controller providing Cu$K\alpha$ radiation. While MnO, Mn_3O_4, and Mn_2O_3 showed X-ray diffraction (XRD) patterns for each single phase, the MnO_2 showed mixed phases of ϵ-MnO_2 and pyrolusite, and the XRD peaks were broader and less intense than those for the other Mn oxides, thus reflecting its higher surface area. The N_2O was either UHP grade or 5090 ppm of N_2O in UHP He (Matheson), and either gas was diluted to the desired concentration with UHP He (MG Ind.). All other gases were UHP grade from MG Industries. BET surface areas were determined by nitrogen adsorption using a QuantaSorb system.

The standard pretreatment before reaction or adsorption experiments was conducted *in situ* in a Pyrex reactor or adsorption cell by exposing the catalyst to He at 1

[1] To whom correspondence should be addressed.

0021-9517/96 $18.00

TABLE 1

Properties of Mn Oxides

Stage	Properties	MnO	Mn_3O_4	Mn_2O_3	MnO_2	MnO_2[a]
A	Color	PG	DB	BL	BL	BL
	Bulk phase	MnO	Mn_3O_4	Mn_2O_4	MnO_2	MnO_2
	Structure	RS	SP	CS	Mixed	Mixed
	SA (m^2/g)	1.5	21.9	34.4	94.7	94.7
B	O_2 release (μmol/g)	—	41	170	2500	—
C	Color	—	DB	BL	BL	BL
	Bulk phase	—	Mn_3O_4	Mn_2O_3	Mn_2O_3	MnO_2
	SA (m^2/g)	—	18.7	31.8	53.3	—
D	Color	BR	DB	BL	BL	BL
	Bulk phase	Mn_3O_4	Mn_3O_4	Mn_2O_3	Mn_2O_3	MnO_2
	SA (m^2/g)	1.0	19.4	28.2	47.3	76.3

Note. A, before pretreatment; B, during pretreatment; C, after pretreatment; D, after reaction, PG, pale green; DB, dark brown; BL, black; BR, brown; RS, rock salt; SP, spinel; CS, C-sesquioxide; mixed, mixture of ϵ-MnO_2 and pyrolusite.

[a] Pretreated at 648 K for 30 min under 10 ml O_2/min.

atm and 30 ml/min. The temperature was raised from room temperature to 393 K, held there for 45 min, then raised to 773 K at a rate of 5 K/min and held there for 90 min. During some of the pretreatment runs, the O_2 released from the Mn oxides was monitored by gas chromatography. Adsorption experiments were carried out using a UHV volumetric adsorption system which has been described elsewhere (38). Equilibrium partial pressures of N_2O up to 200 Torr were used. Two adsorption isotherms for each catalyst sample were taken at each temperature—one for the initial exposure to N_2O and the other following evacuation of N_2O for 30 min at the adsorption temperature after the initial adsorption. Any difference between the two isotherms would represent irreversible uptake of N_2O.

The N_2O decomposition reaction was carried out in a Pyrex reactor containing a preheating section which was immersed in a fluidized sand bath. Typically 0.5 g catalyst was placed on a frit inside the reactor. Concentrations and flow rates (total flow rate 30 ml/min, GHSV 2000 h^{-1}) of the feed gas were governed by Tylan mass flow controllers. The pressure drop across the reactor was about 0.04 atm, most of which was due to the frit. The temperature was measured by a J-type thermocouple inserted in the catalyst bed and was controlled within $\pm 1^\circ$ of the desired temperature by a West 400 temperature controller. It was confirmed that without catalyst no decomposition of N_2O occurs up to 723 K in this reactor. The conversion of N_2O was routinely kept below 10%; i.e., a differential reactor mode was maintained to minimize any complications which may arise from mass and heat transfer limitations. The product analysis was made with a Perkin-Elmer Sigma 3 gas chromatograph equipped with a thermal conductivity detector. A 6′ column of $\frac{1}{8}''$ stainless steel packed with 80/100 mesh 5 Å molecular sieve was used to obtain temperature programmed separation of N_2O, N_2, and O_2. The GC analysis was made 30 min or more after reaction conditions were altered. The conversion of N_2O can be calculated from the concentration of any of the three gases. At steady state, conversions of N_2O based on the different gases agreed very well except in low conversion regions below 1% where the conversion based on N_2O peak differences fluctuated because of analytical error; therefore, the rate of N_2O decomposition was typically based on the N_2 concentration in the product stream.

RESULTS

Three Mn oxides released O_2 during pretreatment, beginning as low as 423 K for MnO_2, 473 K for Mn_2O_3, and 573 K for Mn_3O_4. In all cases the rate of O_2 release first increased then decreased to almost zero toward the end of the pretreatment period. The amount of oxygen released and the changes accompanying the pretreatment are given in Table 1 together with some of the other properties of the Mn oxides. The amount of oxygen released is larger for the more oxidized form of Mn oxides, seemingly reflecting the degree of oxygen lability. Nominal formulae after the standard pretreatment calculated from the amount of oxygen lost for MnO_2, Mn_2O_3, and Mn_3O_4 are $MnO_{1.56}$, $Mn_2O_{2.95}$, and $Mn_3O_{3.98}$, respectively; therefore the pretreatment produced some oxygen vacancies and/or manganese ions of lower oxidation state in Mn_2O_3 and Mn_3O_4. With the standard pretreatment, MnO_2 changed its phase to Mn_2O_3 while losing 40% of its original surface area; hence, MnO_2 was pretreated under 1 atm O_2 at 10 ml/min and 648 K for 30 min, after which no peaks corresponding to Mn_2O_3 were seen in its XRD pattern. The surface areas of Mn_2O_3 and Mn_3O_4 also decreased somewhat during the pretreatment, but their bulk phases were retained.

Since the kinetic experiments were conducted with the catalysts after pretreatment, i.e., with somewhat oxygen-deficient samples, it was important to verify that catalytic N_2O decomposition occurred instead of stoichiometric oxidation of the catalyst by N_2O. Thus the N_2/O_2 ratio in the product stream was monitored during N_2O decomposition over the four different Mn oxides at 0.066 atm of N_2O and temperatures between 573 and 723 K. As shown in Fig. 1, Mn_2O_3 and Mn_3O_4 gave steady catalytic decomposition activity and achieved the stoichiometric N_2/O_2 ratio of 2 quickly, whereas MnO and MnO_2 behaved differently. When N_2O was contacted with MnO at 623 K, it decomposed rapidly to produce N_2 at conversions of 60% or more; however, no O_2 was evolved into the effluent stream. This is not surprising considering that the free energy change at 623 K (calculated assuming constant enthalpies of formation of MnO and Mn_3O_4) strongly favors Mn_3O_4 formation; i.e.,

$$3MnO + N_2O \rightarrow Mn_3O_4 + N_2$$
$$\Delta G(623\ \text{K}) = -72.3\ \text{kcal/mol}\ Mn_3O_4.$$

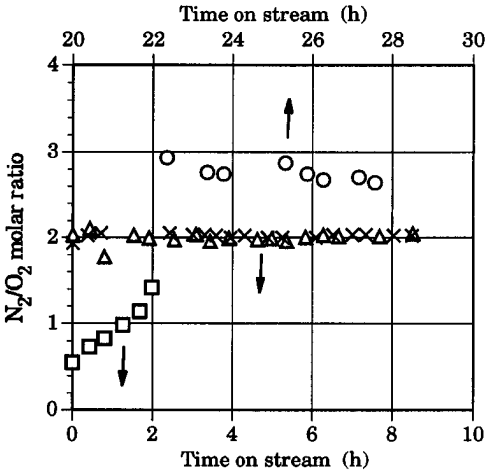

FIG. 1. N_2/O_2 ratio in the effluent gas during N_2O decomposition; $P_{N_2O} = 0.066$ atm, 573 K to 723 K: (○) MnO, (×) Mn_3O_4, (△) Mn_2O_3, (□) MnO_2.

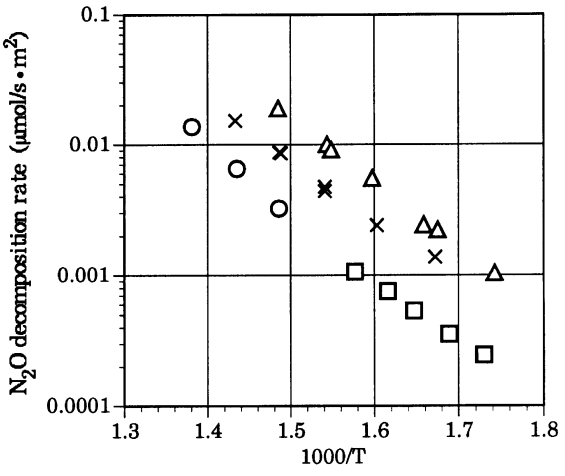

FIG. 2. Arrhenius plots for N_2O decomposition over Mn oxides; $P_{N_2O} = 0.066$ atm: (○) MnO, (×) Mn_3O_4, (△) Mn_2O_3, (□) MnO_2.

The N_2O conversion decreased as time on stream increased, and a gradual increase of O_2 in the product stream was observed. After a 30-h exposure to N_2O, the conversion had fallen to around 2% at 723 K and bulk oxidation to Mn_3O_4 had occurred as confirmed by its brown color and XRD pattern. MnO_2, on the other hand, released oxygen to give N_2/O_2 ratios lower than 2, but no detectable change was observed in its XRD pattern (or those of Mn_2O_3 or Mn_3O_4) after reaction.

The activities for N_2O decomposition over these four Mn oxides were measured over a temperature range from 573 to 698 K and partial pressures of N_2O (P_{N_2O}) ranging from 0.031 to 0.27 atm. The results are given in Table 2 and Fig. 2. Among the four oxides, Mn_2O_3 is most active and gives a specific activity of 4.8×10^{-3} μmol/s · m^2 at 623 K and 0.066 atm N_2O, while Mn_3O_4 shows about half the specific activity of Mn_2O_3. The apparent activation energies are around 20 kcal/mol, and reaction orders with respect to N_2O are less than unity for all the Mn oxides (MnO was not studied). Activity behavior for MnO_2 after the standard pretreatment is also given in Table 2. Interestingly, this MnO_2 sample has almost identical activity, activation energy, and reaction order values compared to those for Mn_2O_3, completely consistent with the fact that the pretreatment converts MnO_2 into Mn_2O_3.

The kinetic behavior was studied further for Mn_2O_3, the most active of the Mn oxides, and the partial pressure effects of the reactants and products were determined. These experiments were conducted following a relatively rapid deactivation during the first 2 h on stream because a much slower activity loss occurred subsequently, as shown in Fig. 3. An activity decrease of only 20% was observed between 2 and 30 h on-stream. The N_2O pressure was varied widely at 623 K and the results are shown in Fig. 4. The reaction order with respect to N_2O is 0.75 in the higher P_{N_2O} region and is 0.84 in the lower region, and with O_2 in the reactant stream the reaction order is still less than unity, i.e., 0.88.

TABLE 2

Kinetic Parameters for N_2O Decomposition over Mn Oxides.

Catalyst	N_2O decomposition rate[a] × 10^4 (μmol/s · g)	(μmol/s · m^2)	SA[b] (m^2/g)	E_a (kcal/mol)	Reaction order
MnO	6.3	6.3	1.0	27	—
Mn_3O_4	490	25	19.4	20	0.89
Mn_2O_3	1400	48	28.2	23	0.78
MnO_2[c]	620	8.1	76.3	19	—
MnO_2	2700	59	47.3	23	0.74

[a] 623 K, $P_{N_2O} = 0.066$ atm.
[b] After reaction.
[c] Pretreated at 648 K for 30 min under 10 ml O_2/min.

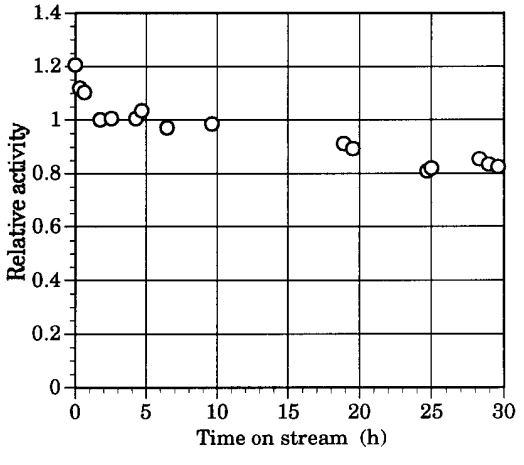

FIG. 3. Activity maintenance during N_2O decomposition over Mn_2O_3: $T = 623$ K; $P_{N_2O} = 0.1$ atm; activity basis, $1 = 0.204$ μmol N_2/s · g.

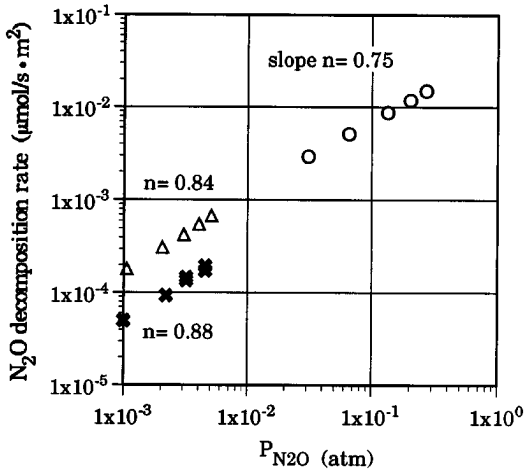

FIG. 4. N_2O partial pressure dependence for N_2O decomposition over Mn_2O_3 (623 K): (○, △) zero P_{O_2} in the feed gas, (×) $P_{O_2} = 0.01$ atm in the feed.

The presence of the products of N_2O decomposition, N_2 and O_2, produce different effects; i.e., N_2 has no effect while O_2 retards the reaction, as found for Mn_2O_3 by Rheaume and Parravano (11). As shown in Fig. 5, the decomposition rate falls by a factor of two as the partial pressure of O_2 increases from zero to 0.04 atm at 648 K. To better model the N_2O decomposition reaction over Mn_2O_3, rate data were taken at five different temperatures between 598 and 648 K, with the N_2O pressure ranging from 0.05 to 0.20 atm, and the O_2 pressure ranging from 0 to 0.08 atm. In the course of the experiment, the activity over Mn_2O_3 gradually decreased by 20% during 30 h on stream, while no noticeable change in surface area was observed. To compensate for this deactivation, experimental points under standard conditions, i.e., $P_{N_2O} = 0.1$ atm at 623 K, were periodically obtained and

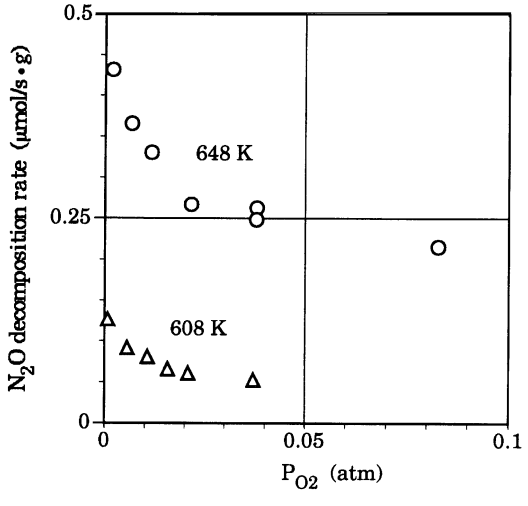

FIG. 5. O_2 partial pressure dependence for N_2O decomposition over Mn_2O_3 ($P_{N_2O} = 0.1$ atm).

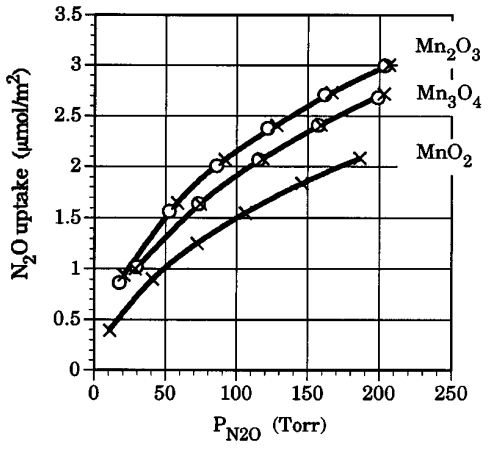

FIG. 6. N_2O adsorption on Mn oxides at 297 K: (○) initial uptake, (×) second uptake.

rates were normalized to the activity at these conditions. The resultant data will be discussed later.

N_2O adsorption isotherms for three of the Mn oxides are given in Fig. 6. The initial uptake and the second uptake on Mn_2O_3 and Mn_3O_4 were essentially identical within experimental uncertainty which means that little or no irreversible adsorption occurred under these conditions. Earlier studies with NiO (12) and Cr_2O_3 (13) reported that some N_2O decomposition occurred, oven at room temperature. Although decomposition might have occurred in the present case, the extent must have been minor in view of the almost identical traces of the initial and the second isotherms. Assuming reversible Langmurian adsorption, saturation monolayer coverages were calculated to be 2.9, 4.0, and 3.8 μmol N_2O/m^2, i.e., 1.7, 2.4, and 2.3×10^{18} molecule/m^2 for MnO_2, Mn_2O_3, and Mn_3O_4, respectively. Moreover, from the adsorption isotherms at 273, 329, and 353 K, ΔH^0_{ad} and ΔS^0_{ad} values for N_2O on Mn_2O_3 were calculated to be -5 kcal/mol and -12 cal/mol · K, respectively, consistent with weak, reversible N_2O chemisorption.

DISCUSSION

Only a limited number of studies have been conducted on N_2O decomposition over Mn_2O_3 and MnO_2 (7–11), and none has been reported using MnO or Mn_3O_4; consequently, the results for only Mn_2O_3 and MnO_2 can be compared to earlier work. Tanaka and Ozaki studied N_2O decomposition over Mn_2O_3 using a recirculation reactor and reported an activation energy of 17 kcal/mol (8), which is a little lower than that obtained here. Extrapolation of their initial rate data to the conditions in Table 3 gives 7.7×10^{-3} μmol/s · m^2 as compared to our value of 4.8×10^{-3} μmol/s · m^2. Considering that the comparison is between steady-state and unsteady-state data, the agreement is quite satisfactory. Moreover, their somewhat larger value is plausible because their initial rate is free from the inhibitory

TABLE 3

Comparison of N_2O Decomposition Activity

Catalyst	Temp. (K)	P_{N_2O} (atm)	N_2O decomp. rate[a] (μmol/s · g) × 10^5	N_2O decomp. rate[a] (μmol/s · m^2) × 10^6	Reference
Mn_2O_3	623	0.066	14,000	4800	This study
Mn_2O_3	623	0.066	—	7700	8
Mn_2O_3 (873)	623	0.066	—	5400	9
Mn_2O_3 (1073)	623	0.066	—	3800	9
Mn_3O_4	623	0.066	4,900	2500	This study
CuO	529	0.066	2,800	—	14
CoO (110)	623	0.066	—	1900	15
Cr_2O_3	623	0.066	380	240	16
MgO	689	0.066	130	—	14
Fe_2O_3/Al_2O_3	623	0.066	25	—	17
ZnO	623	0.066	5	—	18
Fe-Y zeolite	623	0.066	23	—	30
Mn_2O_3	623	0.001	590	180	This study
Mn_3O_4	623	0.001	120	63	This study
La_2O_3	623	0.001	220	650	19
4% Li/MgO	623	0.001	4	12	20
[Fe]-ZSM-5	553[b]	0.001	7,700[c]	—	37
Cu-ZSM-5	623	0.001	13,000	—	4
Rh-ZSM-5	623	0.001	72,000	—	4

[a] Extrapolated to the conditions in the table using the rate data and activation energy in the references assuming a linear partial pressure dependence on N_2O.

[b] Maximum activity around 580 K.

[c] Measured by TPR.

effect of O_2, whereas the steady-state data in this investigation reflect this inhibition. Cimino and Indovina also used a recirculation reactor for N_2O decomposition and reported rate data for two Mn_2O_3 samples prepared from $MnCO_3$ by different methods; i.e., Mn_2O_3 (873) was prepared at 873 K and Mn_2O_3 (1073) was prepared at 1073 K (9). The activation energies reported for Mn_2O_3 (873) and Mn_2O_3 (1073) were 28 and 22 kcal/mol, respectively, while an estimation of rates at the standard conditions used here gives values of 5.4×10^{-3} μmol/s · m^2 for Mn_2O_3 (873) and 3.8×10^{-3} μmol/s · m^2 for Mn_2O_3 (1073), which are close to our results. N_2O decomposition on MnO_2 was studied in a fixed-bed reactor by Kobayashi and Kobayashi (10), and from the rate of 4.7×10^{-3} μmole/s · g at standard conditions and the surface area of 31 m^2, a specific activity of 1.5×10^{-4} μmol/s · m^2 is obtained as compared to our value of 8.1×10^{-4} μmol/s · m^2. One possible reason for this difference is that the surface of MnO_2 in this study was somewhat depleted of oxygen under reaction conditions because the N_2/O_2 ratio in the product gas was lower than stoichiometeric.

Table 3 also compares the N_2O decomposition activity of Mn_2O_3 and Mn_3O_4 with those reported for other oxide catalysts. The rates given in the table are compared at an N_2O pressure of either 0.066 or 0.001 atm by extrapolating data found in the literature. The Mn oxides show much lower activities on a weight basis than those for Cu-ZSM-5 or Rh-ZSM-5 zeolites. Comparison of activities among metal oxides based on either weight or surface area, however, shows that Mn_2O_3 and Mn_3O_4 are positioned in a more active oxide group which includes CoO, CuO, and La_2O_3, while Cr_2O_3, MgO, Li/MgO, Fe_2O_3, and ZnO exhibit much lower specific activities.

N_2O decomposition has been studied for several decades and numerous papers have been published describing this reaction over various oxide catalysts (5–29). Dell *et al.* studied N_2O decomposition over a layer of cuprous oxide on metallic copper (5) and, together with the results from previous studies, showed an apparent relationship between the activity and the semiconductivity of metal oxide catalysts. According to their classification, p-type oxides are most active, n-type the least, and insulators are intermediate. From the experimental observation of an increase in the electrical conductivity for p-type oxides during the catalytic decomposition of N_2O and a decrease for n-type oxides, Hauffe tried to explain the above correlation by a charge-transfer mechanism (23),

$$N_2O_{(g)} + e^- \rightleftharpoons N_2O^-_{(ad)} \quad [1]$$

$$N_2O^-_{(ad)} \rightleftharpoons N_{2(g)} + O^-_{(ad)} \quad [2]$$

$$2O^-_{(ad)} + \rightleftharpoons O_{2(g)} + 2e^- \quad [3]$$

or

$$N_2O_{(g)} + O^-_{(ad)} \rightleftharpoons N_{2(g)} + O_{2(g)} + e^- \rightarrow, \quad [4]$$

in which one of the O_2 desorption steps (either [3] or [4]) was deemed to be the rate-determining step (rds). However, although the desorption step is catalytically important (6), experimental data taken later with various oxides do not support this as a rds except in a few cases (14). Moreover, existence of N_2O^- species on the surface has not been unanimously agreed upon. For instance, Tanaka and Blyholder studied both the photocatalytic and the thermal catalytic decomposition of N_2O on ZnO and found that the kinetics of these two reactions are completely different. Because the photocatalytic reaction data fit their model postulating surface N_2O^- species, they concluded that the thermal catalytic decomposition proceeds via a mechanism without an adsorbed N_2O^- species (18). Borello *et al.* studied the surface complexes of N_2O adsorbed on α-Cr_2O_3 by infrared spectroscopy and learned that the frequencies were drastically different from those of adsorbed NO_2 species, which are isoelectronic with N_2O^-, whereas they were similar to those of NO_2^+ species, which are isoelectronic with N_2O; therefore, they concluded that the adsorbed N_2O must be a molecular species strongly polarized by the surface cation rather than an N_2O^- species (39). As to an O^- species, Shvets and Kazansky observed this species by ESR after adsorption of N_2O on Mo^{+5} on silica gel at 373 K (40). This was later confirmed by Lunsford and co-workers (41); however, no O^- spectrum has been observed after adsorption of N_2O on ZnO. Considering these contradictory results and the difficulty in identifying the surface species, it may be better, in general, to write the reaction mechanism without specifying any charge transfer; however, one thing almost unanimously agreed upon regarding N_2O decomposition over metal oxides is that anion vacancies, or these vacancies along with altervalent cations, are important.

As a natural extension of studies on binary metal oxides, supported metal oxides and mixed oxides have also been investigated, and reviews are available (25, 26). With spinel-type solid solutions and perovskites, one can control electronic and structural parameters, thereby allowing the role of metal ions and their coordination, anion vacancies, and oxygen lability to be examined (26, 27). Egerton *et al.* studied a system of $Cr_xAl_{2-x}O_3$ solid solutions to find that the activity for N_2O decomposition per chromium ion is high when chromium ion concentrations were low, but the activity of simple Cr_2O_3 was the highest on a surface area basis (27). Cimino and Indovina studied the activity of Mn^{3+} and Mn^{4+} dispersed on MgO and MgO–Li_2O and found that Mn^{3+} ions are more active than Mn^{2+} or Mn^{4+} and that oxygen is more loosely held on Mn^{3+}-rich catalysts (9). Some of the catalysts showed higher activity than their nondispersed counterpart, Mn_2O_3, but the activity enhancement was minor. Angeletti *et al.* studied a system of $Co_xMg_{1-x}Al_2O_4$ and showed that Co^{2+} in octahedral coordination is more active for N_2O decomposition than that in tetrahedral coordination (28). Christopher and Swamy examined the N_2O decomposition activity of $La_{1.85}Sr_{0.15}CuO_{4-y}$, which is a superconducting oxide that contains copper in different valence states. From an activity comparison with $CuAlO_2$ and La_2CuO_4 and from XPS results, they concluded that the higher activity of $La_{1.85}Sr_{0.15}CuO_{4-y}$ is due to the presence of copper in mixed valence states along with an abundance of anion vacancies (29).

Most of the above studies with metal oxides have been focused on mechanistic aspects, and none of them presented a drastically higher activity than that of simple binary oxides. Actually, the activity was often lower. Despite all the studies on metal oxides, none has shown activity high enough to be of practical significance; therefore, various zeolites have been studied for N_2O decomposition. Slinkin *et al.* studied the catalytic decomposition of N_2O over H-mordenite and Ni-mordenite (31), while Fu *et al.* and Leglise *et al.* (30, 32) examined activity over FeY zeolite and Fe-mordenite; however, the activities of these zeolites were poor. Some of the cation-exchanged Y zeolites, namely CuY and FeEuY, studied by Aparicio *et al.* showed activity comparable to the most active metal oxides (33). More recently, Li and Armor reported the high activity of cation-exchanged ZSM-5 zeolites for the catalytic decomposition of N_2O, and their activities on a weight basis are almost two orders of magnitude higher than the most active metal oxides (4). An inhibitory effect of O_2 was observed, but it was minor. Chang *et al.* recently studied Ru-NaZSM-5 and Ru-HNaUSY (ultrastable Y) to find the latter is more active, but both zeolites showed substantial decease in activity in the presence of O_2 (34). Panov *et al.* studied N_2O decomposition over Fe-ZSM-5 using a static system and reported that it was much more active than Fe_2O_3 (35). This work has been extended to a study of ferrisilicate and ferrialuminosilicate analogs of ZSM-5 by Sobolev *et al.* (36). Most recently, Chang *et al.* have studied N_2O decomposition over a ferrisilicate analogue of ZSM-5 ([Fe]-ZSM-5) and an Fe-HZSM-5 using TPR, and they found that [Fe]-ZSM-5 is more active than Fe-HZSM-5 (37). Salient features of the [Fe]-ZSM-5 are a high activity at low temperature and enhanced activity in the presence of oxygen. Interestingly, declining activity was observed at 583–673 K during TPR runs from room temperature to 773 K (37).

Rheaume and Parravano studied N_2O decomposition over Mn_2O_3 in a recirculation reactor and obtained a rate expression derived by postulating quasi-equilibrated N_2O adsorption, a rate-determining N_2O decomposition step, and quasi-equilibrated desorption of O_2 (11), i.e.,

$$2\left[N_2O_{(g)} + * \overset{K_{N_2O}}{\rightleftharpoons} N_2O*\right] \qquad [5]$$

$$2\left[N_2O* \overset{k}{\rightarrow} N_{2(g)} + O*\right] \quad \text{(rds)} \qquad [6]$$

$$2O* \overset{1/K_{O_2}}{\rightleftharpoons} O_2 + *, \qquad [7]$$

where $*$ denotes a surface site. The rate equation

$$r = -\frac{dP_{N_2O}}{dt} = Lk\theta_{N_2O} = \frac{aP_{N_2O}}{1 + bP_{N_2O} + cP_{O_2}^{1/2}} \quad [8]$$

represents a simple Langmuir–Hinshelwood unimolecular decomposition model in which $a = LkK_{N_2O}$, $b = K_{N_2O}$, and $c = K_{O_2}^{1/2}$, where K_{N_2O} and K_{O_2} are equilibrium adsorption constants. This expression fit their data well (11). This expression incorporates the inhibitory effect of O_2, which has been observed in the catalytic decomposition of N_2O over most of the metal oxides.

Winter conducted an extensive study of N_2O decomposition over various metal oxides and tried to correlate the activity with the lattice parameter of the metal oxide (6). He had stressed earlier the importance of oxygen lability because the O_2 desorption step can be the rate determining step during the oxygen exchange reaction over many metal oxides (42). The reaction mechanism proposed was the same as that of Rheaume and Parravano; however, the rate expressions used were simplified forms of Eq. [8]; i.e., $r = aP_{N_2O}$ for low partial pressures of N_2O and $r = aP_{N_2O}/P_{O_2}^{1/2}$ for high partial pressures of N_2O. Most of the later investigations of N_2O decomposition over metal oxides, in which detailed investigation of the kinetics was not always made, utilized the integrated form of the latter rate for data reduction. However, other forms of simplified expressions of Eq. [8] have been used, such as $r = aP_{N_2O}/(1 + cP_{O_2}^{1/2})$ when N_2O chemisorption was not appreciable and $r = aP_{N_2O}/(1 + bP_{N_2O})$ when the oxygen exchange reaction was extremely rapid, e.g., at high temperatures (24). Incidentally, few cases have been consistent with reaction [4], which proposes oxygen removal from the catalyst surface directly by gas-phase N_2O (14, 30).

Steady-state N_2O decomposition was not achieved over the MnO and MnO_2 samples used in this study. The temperature range and reaction conditions were such that MnO does not release oxygen acquired from N_2O and is oxidized, while MnO_2 does not retain all its lattice oxygen. Although a slow subsurface oxidation might occur with Mn_2O_3 which can explain its observed slow deactivation, sintering is more likely the reason, and catalytic N_2O decomposition occurs over Mn_2O_3 (and Mn_3O_4) producing stoichiometric N_2/O_2 ratios. Since little oxygen should diffuse from the bulk at the reaction temperatures used here, which are much below the pretreatment temperature, a cyclic redox reaction presumably occurs on the catalyst surface which requires a mechanism for oxygen removal. Different reactions to remove adsorbed oxygen from the surface lead to two basic models (21). In one sequence of elementary steps, gas-phase N_2O reacts with adsorbed oxygen to produce N_2 and O_2 and regenerate a vacant site, i.e., reaction steps [1], [2], and [4]. This model, however, cannot provide a rate expression that explains the inhibitory effect of O_2, regardless of whether step [4] is irreversible or quasi-equilibrated. The other model, which was adopted in this study, is a simple Langmuir–Hinshelwood sequence represented by steps [5]–[7] that was originally proposed by Rheaume and Parravano for Mn_2O_3 (11). This expression embodies the less than unity reaction order with respect to N_2O, the inhibitory effect of O_2, and the absence of any effect due to N_2. Several other models were examined but were discarded because they failed to explain the experimental results.

The derived rate expression, Eq. [8], was fitted to the experimental data using a nonlinear regression scheme in the SAS computer program package on campus. This iterative Gauss–Newton method was employed under the constraint that the three parameters must be positive, and a convergence criterion of 10^{-8} was used. The results, shown in Fig. 7, give an excellent fit to all data. The kinetic and thermodynamic parameters obtained from the fitting, listed in Table 4, have temperature dependencies that behave reasonably, i.e., the rate constant increases and the equilibrium adsorption constants decrease as temperature increases. If the rate parameters at 623 K in the present case are taken

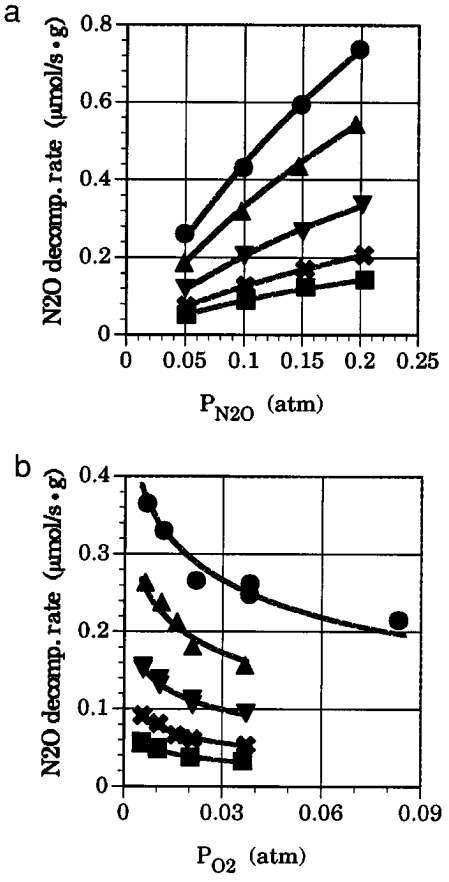

FIG. 7. Fit between model and experimental data for N_2O decomposition over Mn_2O_3: (●) 648 K, (▲) 638 K, (▼) 623 K, (×) 608 K, (■) 598 K. (a) No oxygen in the feed, (b) $P_{N_2O} = 0.1$ atm.

TABLE 4

Model Parameters (from Optimization) for N_2O Decomposition over Mn_2O_3

	Temperature				
	598 K	608 K	623 K	638 K	648 K
K_{N_2O} (atm^{-1})	3.04	2.85	2.80	2.06	2.01
k' ($\mu mol/s \cdot m^2 \times 10^2$)	1.70	2.57	4.29	9.15	12.1
K_{O_2} (atm^{-1})	305	205	158	110	62

as an example, the expression becomes

$$r(\mu \text{ mol/s} \cdot \text{m}^2) = 0.12P_{N_2O}/\left(1 + 2.8P_{N_2O} + 2.8P_{N_2O} + 12.6P_{O_2}^{1/2}\right),$$

and at N_2O and O_2 pressures of 0.1 and 0.04 atm, respectively, the ratio of the three terms in the denominator becomes 1/0.3/2.5, indicating that no terms in the denominator can be neglected. This implies that the oxygen adsorbed on Mn_2O_3 is relatively labile. From the kinetic parameters at different temperatures, as shown in Fig. 8, the activation energy for the rate determining step and the enthalpy and entropy of adsorption for N_2O and O_2, ΔH^0_{ad} and ΔS^0_{ad}, respectively, could be determined. The activation energy for the rds was 31 kcal/mol, while for N_2O adsorption, ΔH^0_{ad} was -7 kcal/mol and ΔS^0_{ad} was -9 cal/mol · K, thus indicating weak N_2O adsorption in agreement with the ΔH^0_{ad} and ΔS^0_{ad} values calculated from the aforementioned adsorption isotherms, which were -5 kcal/mol and -12 cal/mol · K, respectively. The ΔS^0_{ad} values are near the minimum values expected for chemisorption, as discussed by Boudart *et al.* (43) and Vannice *et al.* (44). Finally, for O_2 adsorption (the reverse of step [7]) values of $\Delta H^0_{ad} = -22$ kcal/mol and $\Delta S^0_{ad} = -26$ cal/mol · K were obtained. The study of Mn_2O_3 by Rheaume and Parravano gave values of $\Delta H^0_{ad} = -16.9$ kcal/mol and $\Delta S^0_{ad} = -36.4$ cal/mol · K for N_2O adsorption, and for O_2 adsorption the respective values were -43.2 kcal/mol and -66.0 kcal/mol · K (11). These latter values are considerably larger than ours, whereas their activation energy of 35.0 kcal/mol for the surface reaction is quite similar to our value. A ΔH^0_{ad} value of -24 kcal/mol for O_2 adsorption on Mn_2O_3 was measured calorimetrically by Garner and Ward (45), while an isosteric ΔH^0_{ad} value of -12.2 kcal/mol was determined by Saito from O_2 adsorption isotherms (46). Tanaka and Ozaki reported a ΔH^0_{ad} value of -23 kcal/mol O_2 estimated from a slightly different kinetic model (8). All these enthalpies are closer to that obtained from our rate data. Although a simple sequence, the proposed Langmuir–Hinshelwood model is extremely consistent with all experimental observations and it gives an excellent fit.

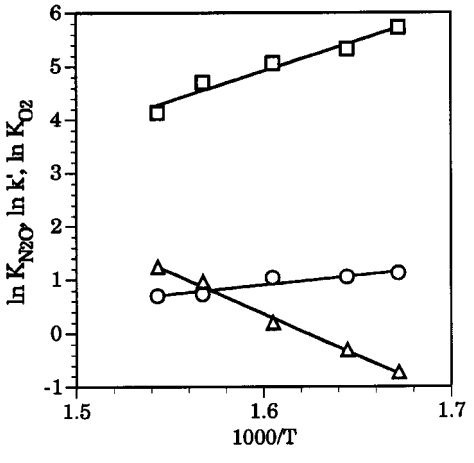

FIG. 8. Estimation of ΔH^0_{ad}, ΔS^0_{ad}, and E_a: (○) K_{NO} (atm^{-1}), (△) k' ($\mu mol/s \cdot g$), (□) $K_{O_2} = (atm^{-1})$.

SUMMARY

Catalytic decomposition of N_2O occurs over all four Mn oxides but stable behavior was observed only for Mn_2O_3 and Mn_3O_4, with the highest specific activity associated with Mn_2O_3. The activities per gram are not as high as those for Cu-ZSM-5 or Rh-ZSM-5, but are rather high for low surface area oxides. Detailed kinetic studies with Mn_2O_3 showed that the reaction order with respect to N_2O is less than unity over a wide concentration range, O_2 inhibits the decomposition, and N_2 has no effect. Chemisorption experiments showed that N_2O weakly adsorbs on Mn_2O_3. A Langmuir–Hinshelwood model fit the kinetic data very well and gave reasonable model parameters which provide adsorption enthalpy and entropy values consistent with thermodynamic criteria and those obtained from adsorption isotherms.

ACKNOWLEDGMENTS

We thank Chemetals for partial support of this study, and one of us (T.Y.) thanks Lion Akzo Co., Ltd., for a grant to study at Penn State. Partial support from Mobil Corporation is also gratefully acknowledged.

REFERENCES

1. Kung, H. H., "Transition Metal Oxides: Surface Chemistry and Catalysis," p. 153. Elsevier, 1989.
2. Thiemens, M. H., and Trogler, W. C., *Science* **251**, 932 (1991).
3. Amand, L. E., Leckner, B., and Andersson, S., *Energ. Fuel* **5**, 815 (1991).
4. Li, Y., and Armor, J. N., *Appl. Catal. B* **1**, L21 (1992).
5. Dell, R. M., Stone, F. S., and Tiley, P. F., *Trans. Faraday Soc.* **49**, 201 (1953).
6. Winter, E. R. S., *J. Catal.* **15**, 144 (1969).
7. Winter, E. R. S., *J. Catal.* **19**, 32 (1970).
8. Tanaka, K., and Ozaki, A., *Bull. Chem. Soc. Jpn.* **40**, 420 (1967).
9. Cimino, A., and Indovina, V., *J. Catal.* **17**, 54 (1970).
10. Kobayashi, M., and Kobayashi, H., *J. Chem. Eng. Jpn.* **6**, 438 (1973).
11. Rheaume, L., and Parravano, G., *J. Phys. Chem.* **63**, 264 (1959).

12. Guilleux, M.-F., and Imelik, B., *Bull. Soc. Chim.* **1310** (1970).
13. Zecchina, A., Cerruti, L., and Borrelo, E., *J. Catal.* **25**, 55 (1972).
14. Kobayashi, H., and Hara, K., *in* "Catalysis under Transient Conditions" (A. T. Bell and L. L. Hegedus, Eds.), p. 163. ACS Symp. Ser., 1985.
15. Volpe, M. L., and Reddy, J. F., *J. Catal.* **7**, 76 (1967).
16. Tanaka, K., and Ozaki, A., *J. Catal.* **8**, 307 (1967).
17. Pomonis, P., Vattis, D., Lycourghiotis, A., and Kordulis, C., *J. Chem. Soc., Faraday Trans. 1* **81**, 2043 (1985).
18. Tanaka, K., and Blyholder, G., *J. Phys. Chem.* **75**, 1037 (1971).
19. Zhang, X., Walters, A. B., and Vannice, M. A., *Appl. Catal. B* **4**, 237 (1994).
20. Zhang, X., Walters, A. B., and Vannice, M. A., *J. Catal.* **146**, 568 (1994).
21. Winter, E. R. S., *Discuss. Faraday Soc.* **28**, 183 (1959).
22. Read, J., *J. Catal.* **28**, 428 (1973).
23. Hauffe, K., *Adv. Catal.* **7**, 213 (1955).
24. Vannice, M. A., Walters, A. B., and Zhang, X., *J. Catal.* **159**, 119 (1996).
25. Larsson, R., *Catal. Today* **4**, 235 (1989).
26. Swamy, C. S., and Christopher, J., *Catal. Rev.-Sci. Eng.* **34**, 409 (1992).
27. Egerton, T. A., Stone, F. S., and Vickerman, J. C., *J. Catal.* **33**, 299 (1974); Ibid. 307 (1974).
28. Angeletti, C., Cimino, A., Indovina, V., Pepe, F., and Shiavello, M., *J. Chem. Soc. Faraday Trans. 1* **77**, 641 (1981).
29. Christopher, J., AND Swamy, C. S., *J. Mol. Cat.* **62**, 69 (1990).
30. Fu, C. M., Korchack, V. N., and Hall, W. K., *J. Catal.* **68**, 166 (1981).
31. Slinkin, A. A., Lavrovskaya, T. K., Mishin, I. V., and Rubinshtein, A. M., *Kinet. Catal.* **19**, 734 (1978).
32. Leglise, J., Petunchi, J. O., and Hall, W. K., *J. Catal.* **86**, 392 (1984).
33. Aparicio, L. M., Ulla, M. A., Millman, W. S., and Dumesic, J. A., *J. Catal.* **110**, 330 (1988).
34. Chang, Y. -F., McCarty, J. G., Wachsman, E. D., and Wong, V. L., *Appl. Catal. B* **4**, 283 (1994).
35. Panov, G. I., Sobolev, V. I., and Kharitonov, A.S., *J. Mol. Catal.* **61**, 85 (1990).
36. Sobolev, V. I., Panov, G. I., Kharitonov, A. S., Romannikov, V. N., Volodin, A. M., and Ione, K. G., *J. Catal.* **139**, 435 (1993).
37. Chang, Y.-F., McCarty, J. G., and Zhang, Y. L., *Catal. Lett.* **34**, 163 (1995).
38. Seyedmonir, S. R., Strohmayer, D. E., Geoffroy, G. L., and Vannice, M. A., *Adsorption Sci. Technol.* **1**, 253 (1984).
39. Borello, E., Cerruti, L., Ghiotti, G., and Guglleminotti, E., *Inorg. Chim. Acta* **6**, 45 (1972).
40. Shvets, V. A., and Kazansky, V. B., *J. Catal.* **25**, 123 (1972).
41. Lunsford, J. H., *Catal. Rev.* **8**, 135 (1973).
42. Winter, E. R. S., *J. Chem. Soc., (A) Inorg. Phys. Theor.* 2889 (1968).
43. Boudart, M., Mears, D. W., and Vannice, M. A., *Ind. Chim. Belge* **32**, (special issue), 281 (1967).
44. Vannice, M. A., Hyun, S. H., Kalpacki, B., and Liau, W. C., *J. Catal.* **56**, 358 (1979).
45. Garner, W. E., and Ward, T., *J. Chem. Soc.* **837**, (1939).
46. Saito, J., *J. Chem. Soc. Jpn.* **72**, 262 (1951).